

Article

Assessment of Heavy Metal(loid) Pollution and Human Health Risks Associated with a Mineral (Zn, Cu, and Sn Ores) Processing Plant in Yunnan, Southwest China

Wenping Luo^{1,2}, Yan Zhang^{1,2,*}, Pingtang Wei^{3,*} and Chengshuai Sun^{1,2}

¹ Faculty of Land Resources Engineering, Kunming University of Science and Technology, Kunming 650093, China; luowen9967@163.com (W.L.); 15667635897@163.com (C.S.)

² South-West Institute of Geological Survey, Geological Survey Center for Nonferrous Metals Resources, Kunming 650093, China

³ Kunming Geological Exploration Institute of China Metallurgical Geology Bureau, Kunming 650024, China

* Correspondence: 20190021@kust.edu.cn (Y.Z.); weipingtang@163.com (P.W.)

Abstract: Understanding the contamination and sources of heavy metal(loid)s (HMs) at historical sites is vital for safeguarding human health and the ecological environment. This study focused on As, Hg, Cd, Cu, Pb, Ni, and Cr concentrations in the residual soil, groundwater, and surface water around a mineral processing plant. The sources of these elements and the human health risks posed by them were evaluated using various indexes. Soil HM concentrations exceeded background values for Yunnan Province, ranked as As > Pb > Cd > Cu > Hg > Ni. The river water met China's Class II waterbody standard; however, Cd, Cu, Pb, and pH exceeded the maximum permissible sewage discharge concentrations in the accumulated water. The groundwater showed severe HM pollution, meeting China's Class III water quality standard. The average value of the Nemerow pollution index was consistent with that of the single-factor pollution index in the following order: As > Pb > Cd > Ni > Cu > Hg. Children face heightened risk through the oral ingestion of As, Cd, and Pb, particularly in high-value sampling points in the residue deposit area. The main sources of these pollutants are anthropogenic activities and the soil formation matrix.

Keywords: construction residual soil; pollution index evaluation; health risk assessment; historical site; mineral processing plant; Yunnan; China



Citation: Luo, W.; Zhang, Y.; Wei, P.; Sun, C. Assessment of Heavy Metal(loid) Pollution and Human Health Risks Associated with a Mineral (Zn, Cu, and Sn Ores) Processing Plant in Yunnan, Southwest China. *Minerals* **2024**, *14*, 253. <https://doi.org/10.3390/min14030253>

Academic Editor: Carlito Tabelin

Received: 31 January 2024

Revised: 23 February 2024

Accepted: 26 February 2024

Published: 28 February 2024



Copyright: © 2024 by the authors. Licensee MDPI, Basel, Switzerland. This article is an open access article distributed under the terms and conditions of the Creative Commons Attribution (CC BY) license (<https://creativecommons.org/licenses/by/4.0/>).

1. Introduction

Heavy metal(loid) (HM) pollution has become a global environmental problem due to its irreversibility, invisibility, persistence, and non-degradability. Over 10 million contaminated sites worldwide are polluted by HMs [1–3]. With the rapid development of China's social economy, 'brownfields' left behind by the relocation of industrial and mining relocations are now contaminated by HMs. The direct development and utilization of untreated contaminated sites will pose a threat to the surrounding environment and the health of residents [4,5]. The chemical manufacturing industry is an important anthropogenic source of HMs in 625 industrial zones in China [6,7], especially in areas where nonferrous metals are smelted, posing a significant environmental risk to the surrounding areas [8–11].

Studies have shown that HM pollution adversely affects human health and the environment, and industrial waste causes environmental degradation [12,13]. HMs are susceptible to further diffusion into the groundwater through leaching and seepage [14,15]. For example, mining and processing enterprises may cause the environmental pollution of the surrounding soil during operation [16–18] or shutdown [19]. Peng et al. [20] found that soils around 40 copper smelting sites in China were polluted by a variety of HMs including Cr, Pb, Cd, Zn, Ni, and As, the soil was slightly acidic [21], and significant groundwater contamination occurred [22]. The water was highly contaminated by Cr

and Pb [23]. As [24,25], Pb [26], and Cd [27] pose health risks to humans. Therefore, it is particularly important to objectively evaluate the pollution characteristics and ecological risks of HMs at historical sites and identify their migration and enrichment pathways. Such information will serve as a reference for subsequent scientific development and utilization.

Southwest China has abundant mineral resources leading to the functioning of mining and smelting industries and other related activities that cause HM pollution of the soil [28,29]. Yunnan is rich in nonferrous metal deposits and associated mining, smelting, and beneficiation (rock breaking, ore transportation, ore processing) activities. HMs not only damage the surrounding soil through surface water and groundwater seepage and other pathways [30,31], but also cause harm to human health by entering the food chain through agricultural products. Studies on the soil in Yunnan [32–34] show varying degrees of HM pollution, emphasizing the importance of evaluating HM pollution originating from the residual land of the mineral processing plant.

This study focused on a historical mineral processing site in Yunnan Province assessing the HM pollution status in the residue soil, surface water, and groundwater based on the site of the environmental investigation, assessed the health risk of the HM exposure of the population based on the U.S. Environmental Protection Agency's (EPA's) Health Risk Model, and used correlation analysis to identify the source of the HMs. The findings of this study are expected to provide a theoretical foundation for the effective management and control of residual soil in this area. Additionally, such information will serve as a theoretical reference for determining the suitability of transforming the abandoned site from industrial to residential land.

2. Materials and Methods

2.1. Overview of the Study Area

The study area is located 66 km from Xichou County and approximately 20 m away from the river, which is primarily surrounded by forest and farmland. It houses a historic Zn, Cu, and As beneficiation plant, with the nearest villages, Village 1 and Village 2, located directly east of the site at a straight line distance of 760 m and southwest of the site at a straight line distance of 805 m, respectively. Approximately 1000 residents reside around the site, which was formerly a mining area and is now slated for conversion to construction land.

The site extends in a northeast–southwest direction, covering an area of 24,738.4 m², comprising residue deposits, raw ore yards, workshops, laboratories, sedimentation tanks, dewatering tanks, and timber mills. The hydrogeological conditions are complex, and surface water is abundant at the sites and surrounding areas. Currently, there is a lack of implemented remediation measures, leading to the haphazard stacking of waste residue and incomplete dismantling of workshops. The unmanaged waste residue is subjected to adverse weather conditions, including rainwater washing, groundwater migration, and soil exposure. As a result, soil, groundwater, and surface water in the area are significantly contaminated. Surface water, particularly laden with slag, exhibits predominant discoloration such as brownish-red and red hues, emitting a strong and unpleasant odor within the mineral processing plant.

The landform in the study area is classified as a karst plateau peak cluster in southeastern Yunnan. The climate is warm, rainfall is abundant, and the tectonic superposition is complex and active. The main lithology from the top to bottom are the Quaternary reclamation soil layer (Q₄^{ml}), Quaternary alluvial–diluvial layer (Q₄^{al+pl}), and Middle Cambrian Tianpeng Formation (E₂t). The rocks consist of strongly weathered muddy siltstone and moderately weathered limestone, which are primarily composed of quartz, feldspar, mica, and calcite. Owing to the interaction of climate, biology, and topography, a variety of soil types are present in the study area, including red, yellow, yellow-brown, purple, red, limestone, and paddy soils. The soil pH is neutral (Accessed 20 December 2023: China Soil Database, <http://vdb3.soil.csdb.cn/>).

2.2. Sampling and Analyses

2.2.1. Sample Collection

(1) Soil

Adhering to the China’s “Technical Guidelines for Soil Environmental Investigation and Assessment of Construction Land”, the suspected contaminated areas were screened through pollution identification and preliminary investigations. A minimum of one sample per 400 m² was collected in potentially contaminated areas. One sample per 1600 m² was collected in other areas.

In adherence to the China’s “Technical Guidelines for Environmental site Monitoring” (HJ25.2-2014) [35], the determination of vertical sampling depth involved subtracting the thickness of the surface unconsolidated soil layer. The prescribed sampling depth was set at 10 m or extended to the strongly weathered rock layer. For deep soil, sampling intervals were designated as 0.5 m within 3 m, 1 m for depths of 3–6 m, and 2 m for depths exceeding 6 m. However, the actual sampling depth was 1–13 m, utilizing the multi-point sampling method (Figures 1 and 2) to remove impurities such as lant roots and gravel. Approximately 1 kg of soil samples was collected in a sample bag. After drying naturally, the soil samples were crushed using a wooden stick and passed through a 2 mm aperture sieve. The preprocessed soil was mixed and homogenized, weighed, and then sent to the laboratory for analysis.

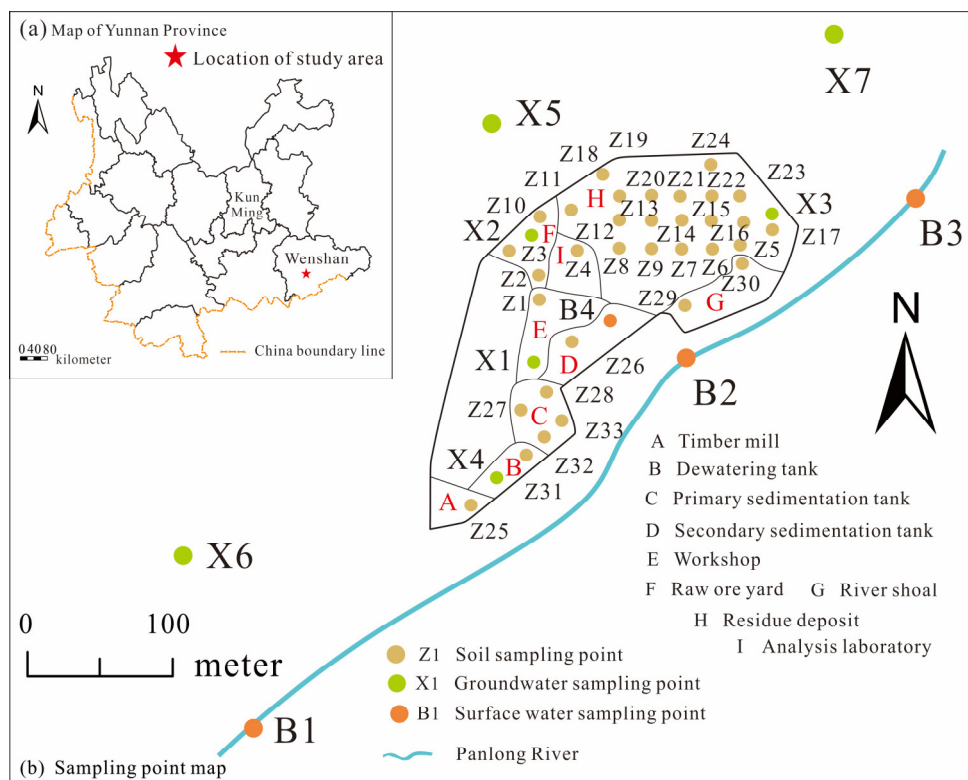


Figure 1. Location of the sampling sites. (a) Location of the study area. (b) Extent of the study area and distribution of sampling points.

(2) Surface water

In accordance with the China’s “Technical Specifications Requirements for Monitoring of Surface Water and Waste Water”(HJ-T91-2002) [36], the selection of monitoring sections was designed to holistically represent the quality of the aqueous environment or the surrounding region on a general or macro scale.

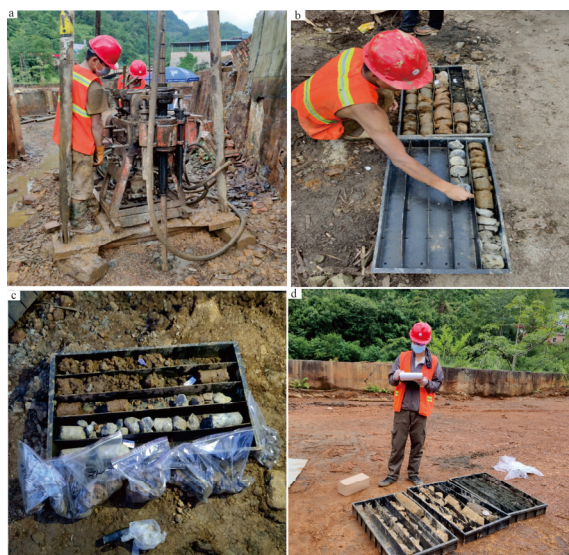


Figure 2. Sampling pictures.

One sampling site was strategically placed in the sediment pond with the highest water accumulation (Point B4). Three surface water samples (Points B1, B2, B3) were collected from the upper, middle, and lower reaches of the Panlong river. Before storing the samples, checks were performed for the integrity of the bailers and intact fittings. They were then washed and soaked with nitric acid ($c = 1 \text{ mol/L}$) for 1 to 2 days and then rinsed with distilled or deionized water before adding the necessary protective agent (concentrated nitric acid) [37]. Subsequently, all samples were filtered through a $0.45\text{-}\mu\text{m}$ filter membrane, followed by acidification with nitric acid to $\text{pH} \leq 2$, stored below $4 \text{ }^\circ\text{C}$, and promptly transported to the laboratory.

(3) Groundwater

Four groundwater monitoring wells were deployed along the direction of groundwater flow (Points X1, X2, X3, X4). Control monitoring wells were established in each of the north, west, and south directions of the site (Points X5, X6, X7). Water was sampled at 0.5 m below the water surface in the monitoring wells.

Groundwater samples were promptly collected within 2 h after well washing, utilizing designated bailers. Each monitoring well contributed one groundwater sample, which was immediately transferred into pre-prepared sample bottles containing the requisite protective agent. The samples were then placed in a specially designed re-frigerated box, maintained at a temperature of $4 \text{ }^\circ\text{C}$, protected from light, and promptly dispatched to the laboratory for analysis within their respective preservation periods.

2.2.2. Sample Analysis and Testing

The analysis of HM samples was conducted at the Kunming Geological Exploration Institute of the China Metallurgical Geology General Administration. During the determination of HM content, stringent control measures were implemented. The blank standard addition recovery rate was set within 90–110%, the sample standard addition recovery rate was 70–130%, and the relative deviation of parallel samples in the laboratory was controlled at 20%. Furthermore, the absolute deviation of pH was 10% (0.1 pH). These controls adhere to the China's "Technical Specification for Soil Environmental Monitoring" (HJ/T166-2004) [38]. For detailed testing and analysis methods, refer to Supplementary Material Table S1.

2.3. Evaluation Methods

2.3.1. Evaluation of Pollution Degree of Site

The assessment of HM pollution status and the comprehensive pollution degree of soil and water resources in the study area utilized screening values from GB 15618-2018 China's "Soil Environmental Quality Construction Land Soil Pollution Risk Control Standard" [39], in conjunction with the single-factor pollution index (P_1) [40–42] and Nemerow pollution index (P_N) [43–46]. Specific values are detailed in Tables S2 and S3.

2.3.2. Human Health Risk Assessment

Human health risk assessments delineate the potential hazards of various HMs to human health [47]. Adopting the American Superfund Risk Assessment Guide [48] and informed by the related research, a calculation formula for health risk assessment was derived. Subsequently, the soil health risk in the study area was evaluated (Tables S4 and S5).

3. Results and Discussion

3.1. Characteristics of HM Pollution

3.1.1. Soil

As shown in Table 1, the field-measured average pH value was 5.91, indicating weak acidity in the study area. The average concentrations of HMs in the soil exceeded the respective background values of the soil environment in Yunnan Province [49] by 132.66 and 85.68 times for As and Cd, respectively. The over-standard rates of the samples were 89.72% and 87.94% for As and Cd, respectively. Based on the screening values obtained from the China's "Soil Environmental Quality Construction Land Soil Pollution Risk Control Standard" (GB 36600-2018), some HMs exceeded the prescribed limits. As, Cd, and Pb exceeded the screening values in 7.80, 4.26, and 6.74% of the total samples, respectively. The remaining elements did not exceed the standard. Notably, As exceeded the control value in 59.57% of the samples. The coefficient of variation (CV) reflects the spatial dispersion and variability of HMs, with a higher CV indicating a greater influence of anthropogenic factors [50]. In the study area, the order of CV values was As > Pb > Cd > Cu > Hg > Ni. Except for Ni, all other elements had values > 1, indicating significant spatial variations and potential anthropogenic pollution.

Table 1. Characterization of soil heavy metal(loid) content in the study area ($\text{mg}\cdot\text{kg}^{-1}$).

Characteristic Parameter	pH	As	Hg	Cd	Cu	Ni	Pb
Min	2.65	3.55	0.002	0.01	1.83	2.62	1.08
Max	8.91	24400.0	0.20	244.0	2074.0	132.0	1966.0
Avg	5.91	2441.0	0.04	18.85	313.08	30.56	215.39
SD	-	4917.59	0.04	31.73	432.57	22.44	369.53
CV	-	2.01	1.01	1.68	1.38	0.73	1.72
Background value of Yunnan Province	background value	18.40	0.058	0.22	46.30	42.50	40.60
	Beyond the number	253	56	248	190	95	194
	excessive rate	89.72%	19.86%	87.94%	67.38%	33.69%	68.79%
	Excess multiples	132.66	0.69	85.68	6.76	0.72	5.31
Soil pollution of construction land	screening values	60	38	65	18000	900	800
	Beyond the number	22	0	12	0	0	19
	excessive rate	7.80%	0	4.26%	0	0	6.74%
	Excess multiples	40.68	0.001	0.29	0.02	0.03	0.27
Risk management and control standards	Control value	140	82	172	36000	2000	2500
	Beyond the number	168	0	1	0	0	0
	excessive rate	59.57%	0	0.35%	0	0	0
	Excess multiples	17.44	0.0005	0.11	0.009	0.02	0.09

Note: All samples of Cr are below the detection limit. The number of exceedances refers to the number of measured contents higher than the background, screening, and control values in Yunnan Province. excessive rate = the number of exceedances / the total number of measurements, Excess multiples = the average value of each element / the background, screening, and control values in Yunnan Province.

3.1.2. Surface Water

In accordance with the site's future planning, the river water quality must meet the requirements of China's Class II. The evaluation of the river surface water samples adhered to the China's "Surface Water Environmental Quality Standard" (GB3838-2002) [51], and the HMs did not exceed the standard limits. However, the accumulated water (Point B4) at the site was appraised against the maximum allowable emission concentration standard values outlined in the China's "Integrated Wastewater Discharge Standard" (GB8978-1996) [52]. The concentrations of As, Cd, and Cu, as well as pH values exceeded the permissible limits (Table 2). This deviation is attributed to the influence of waste residue and contaminated soil on the water accumulation at the site. Prolonged water immersion facilitates the leaching of toxic substances, resulting in concentrations that exceed the standard limits.

Table 2. HM pollution concentrations in surface water and groundwater.

Types	Sample Number	pH	As	Hg	Cr	Cd	Cu	Ni	Pb
Surface water (mg·L ⁻¹)	B1	8.17	0.0099	<0.00004	<0.004	<0.00005	0.0005	0.0002	0.0001
	B2	8.21	0.0088	<0.00004	<0.004	<0.00005	0.0006	0.0001	0.0001
	B3	8.21	0.0078	<0.00004	<0.004	<0.00005	0.0011	0.0005	0.0002
	Standard limit	6~9	0.05	0.00005	0.05	0.005	1.00	-	0.01
	B4	2.49	0.953	<0.00004	<0.004	0.257	2.061	0.0566	0.0116
	Standard limit	6~9	0.5	0.05	0.5	0.1	0.5	1.0	1.0
Groundwater (mg·L ⁻¹)	standard limit	6.5~8.5	≤0.01	≤0.001	≤0.05	≤0.005	≤1.0	≤0.02	≤0.01
	X1	6.1	0.93	<0.00004	0.009	0.00128	0.001	0.0365	0.0005
	X2	4.43	0.454	<0.00004	0.01	0.184	0.703	0.0507	0.0028
	X3	6.98	0.056	<0.00004	0.011	0.00118	0.00062	0.0017	0.0004
	X4	5.66	0.256	<0.00004	0.009	0.00271	0.0144	0.0028	0.0006
	X5	7.62	0.009	<0.00004	<0.004	0.00014	0.0008	<0.00006	<0.00009
	X6	7.19	0.0038	<0.00004	0.008	0.000006	0.0002	0.0002	<0.00009
	X7	7.73	0.0085	<0.00004	0.012	<0.00005	0.0006	<0.00006	<0.00009

3.1.3. Groundwater

According to the China's "Groundwater Quality Standard" (GB/T14848-2017) [53] (Class III), the average mass concentration of HMs follows the sequence: As > Cu > Cd > Ni > Cr > Pb > Hg. The pH values of monitoring points X1, X2, and X4 exceeded the prescribed standards. The sequence of multiple points surpassing the standard limits is X1 (93 times) > X4 (45.4 times) > X4 (25.6 times) > X3 (5.6 times) for As, and X2 (2.5 times) ≥ X1 (1.825 times) for Ni, and X2 (36.8 times) for Cd. On the contrary, the HMs in monitoring wells X5, X6, and X7 were lower than the Class III water quality standard for groundwater (Table 2). This discrepancy suggests that when the soil is polluted, harmful substances may be transferred to the groundwater through atmospheric precipitation, leading to an increase in harmful substances in the groundwater and subsequent pollution.

3.2. Evaluation of the HM Pollution Index

The single-factor pollution index and Nemerow pollution index method were used to evaluate six HMs in the residual soil of the study area (Table 3). The average Pi values were ranked in the following order: As (40.68) > Pb (1.77) > Cd (0.85) > Ni (0.11) > Cu (0.05) > Hg (0.004). Analysis of the pollution levels revealed that As pollution was the most severe, with the samples accounting for 58%. Conversely, the other samples did not exhibit severe pollution. The proportions of moderate pollution samples for As and Pb were 4% and 1%, respectively. All the samples of Hg, Cu, and Ni were uncontaminated (Figure 3). The average values of PN were consistent with Pi, with Cd almost reaching the warning level, warranting attention in subsequent stages.

Table 3. Pollution index of HMs in soil.

Pollution Index	P _i					
	As	Hg	Cd	Cu	Ni	Pb
Min	0.06	0.00005	0.0002	0.0001	0.003	0.001
Max	406.67	0.005	3.75	0.12	0.15	2.46
Avg	40.68	0.0009	0.29	0.02	0.03	0.27
P _N	291.01	0.004	0.85	0.05	0.11	1.77
Degree pollution	High pollution	Uncontaminated	Warning Level of Caution	Uncontaminated	Uncontaminated	Light pollution

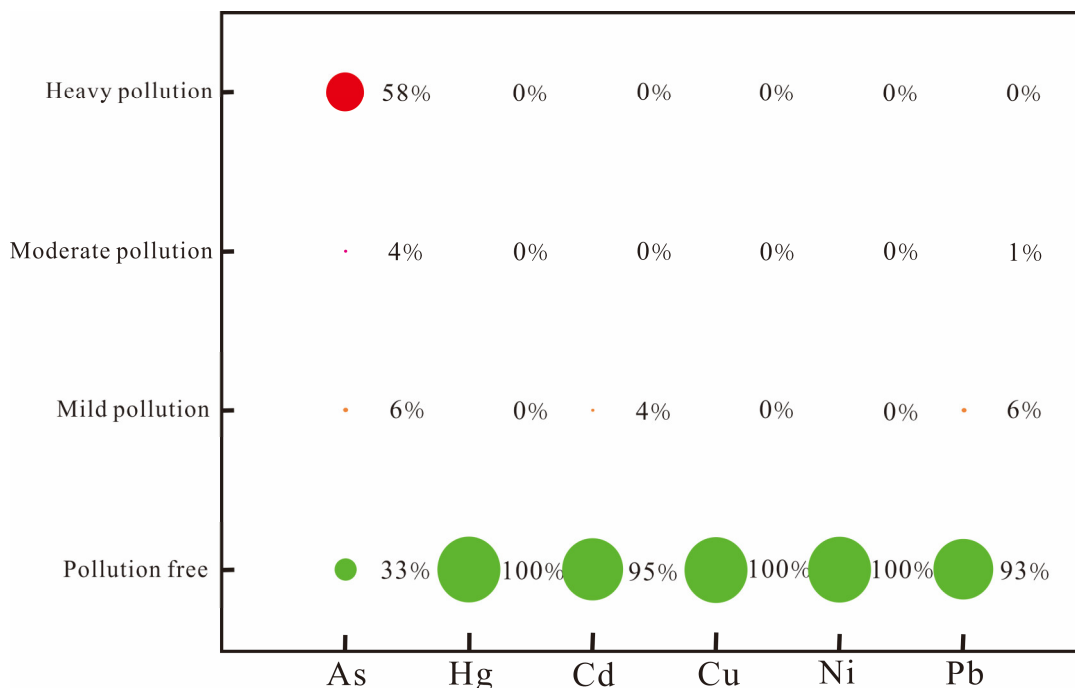


Figure 3. Proportion of soil heavy metal(loid) single factor index pollution.

3.3. Human Health Risk Assessment

Soil HMs primarily enter the human body through oral intake, respiratory inhalation, and skin contact [54]. Non-carcinogenic (hazard quotient) and carcinogenic risks are denoted for each HM by HQ and CR, respectively. The hazard index (HI) represents the cumulative potential non-CR posed by each HM through different pathways [55]. The acceptable range for CR is set between 1.0×10^{-6} and 1.0×10^{-4} . $CR > 1.0 \times 10^{-4}$, is considered high. When HQ and HI are <1 , there is no HQ. Conversely, HQ is present when HQ and HI exceed 1 [56].

3.3.1. Exposure Risk Assessment

In the residual soil of the study area, the exposure parameters of the health risk assessment model were employed to calculate the average daily intake of carcinogenic and non-carcinogenic HMs in adults and children (Table 4). The order of average daily intake for both carcinogenic and non-carcinogenic exposure pathways in adults and children is $ADD_{ing} > ADD_{inh} > ADD_{derm}$, with oral intake identified as the primary route for both adults and children. Notably, children exhibit a higher exposure than adults. In the CR exposure pathway, the oral intake pathway poses a higher risk for children compared to adults, whereas skin contact and respiratory inhalation are higher for adults than for children. Conversely, in the HQ exposure pathway, children exhibit higher exposure than adults.

Table 4. Average daily exposure of soil HMs causing cancer (mg·(kg·d)⁻¹).

HMs	ADD _{ing}		ADD _{derm}		ADD _{inh}		ADD		
	Adult	Child	Adult	Child	Adult	Child	Adult	Child	
Carcinogenic	As	1.41 × 10 ⁻³	2.52 × 10 ⁻³	1.51 × 10 ⁻⁷	6.96 × 10 ⁻⁸	5.64 × 10 ⁻⁵	7.07 × 10 ⁻⁵	1.47 × 10 ⁻³	2.60 × 10 ⁻³
	Hg	2.05 × 10 ⁻⁸	3.66 × 10 ⁻⁸	2.19 × 10 ⁻¹²	1.01 × 10 ⁻¹²	8.18 × 10 ⁻¹⁰	1.03 × 10 ⁻⁹	2.13 × 10 ⁻⁸	3.76 × 10 ⁻⁸
	Cd	1.09 × 10 ⁻⁵	1.95 × 10 ⁻⁵	1.16 × 10 ⁻⁹	5.37 × 10 ⁻¹⁰	4.35 × 10 ⁻⁷	5.46 × 10 ⁻⁷	1.13 × 10 ⁻⁵	2.00 × 10 ⁻⁵
	Cu	1.81 × 10 ⁻⁴	3.24 × 10 ⁻⁴	1.93 × 10 ⁻⁸	8.93 × 10 ⁻⁹	7.23 × 10 ⁻⁶	9.06 × 10 ⁻⁶	1.88 × 10 ⁻⁴	3.33 × 10 ⁻⁴
	Ni	1.77 × 10 ⁻⁵	3.16 × 10 ⁻⁵	1.89 × 10 ⁻⁹	8.71 × 10 ⁻¹⁰	7.06 × 10 ⁻⁷	8.85 × 10 ⁻⁷	1.84 × 10 ⁻⁵	3.25 × 10 ⁻⁵
	Pb	1.25 × 10 ⁻⁴	2.23 × 10 ⁻⁴	1.33 × 10 ⁻⁸	6.14 × 10 ⁻⁹	4.97 × 10 ⁻⁶	6.24 × 10 ⁻⁶	1.30 × 10 ⁻⁴	2.29 × 10 ⁻⁴
	ADD	1.75 × 10 ⁻³	3.12 × 10 ⁻³	1.86 × 10 ⁻⁷	8.61 × 10 ⁻⁸	6.97 × 10 ⁻⁵	8.74 × 10 ⁻⁵	1.82 × 10 ⁻³	3.21 × 10 ⁻³
Non-carcinogenic	As	4.12 × 10 ⁻³	2.94 × 10 ⁻²	4.39 × 10 ⁻⁷	8.12 × 10 ⁻⁷	1.64 × 10 ⁻⁵	8.24 × 10 ⁻⁵	4.14 × 10 ⁻³	2.95 × 10 ⁻²
	Hg	5.98 × 10 ⁻⁸	4.27 × 10 ⁻⁷	6.37 × 10 ⁻¹²	1.18 × 10 ⁻¹¹	2.39 × 10 ⁻¹⁰	1.20 × 10 ⁻⁹	6.00 × 10 ⁻⁸	4.28 × 10 ⁻⁷
	Cd	3.18 × 10 ⁻⁵	2.27 × 10 ⁻⁴	3.39 × 10 ⁻⁹	6.27 × 10 ⁻⁹	1.27 × 10 ⁻⁷	6.37 × 10 ⁻⁷	3.20 × 10 ⁻⁵	2.28 × 10 ⁻⁴
	Cu	5.29 × 10 ⁻⁴	3.78 × 10 ⁻³	5.64 × 10 ⁻⁸	1.04 × 10 ⁻⁷	2.11 × 10 ⁻⁶	1.06 × 10 ⁻⁵	5.31 × 10 ⁻⁴	3.79 × 10 ⁻³
	Ni	5.16 × 10 ⁻⁵	3.69 × 10 ⁻⁴	5.50 × 10 ⁻⁹	1.02 × 10 ⁻⁸	2.06 × 10 ⁻⁷	1.03 × 10 ⁻⁶	5.18 × 10 ⁻⁵	3.70 × 10 ⁻⁴
	Pb	3.64 × 10 ⁻⁴	2.60 × 10 ⁻³	3.88 × 10 ⁻⁸	7.16 × 10 ⁻⁸	1.45 × 10 ⁻⁶	7.27 × 10 ⁻⁶	3.65 × 10 ⁻⁴	2.61 × 10 ⁻³
	ADD	5.10 × 10 ⁻³	3.64 × 10 ⁻²	5.43 × 10 ⁻⁷	1.00 × 10 ⁻⁶	2.03 × 10 ⁻⁵	1.02 × 10 ⁻⁴	5.12 × 10 ⁻³	3.65 × 10 ⁻²

Note: The ADD is defined as average exposure dose for each pathway.

3.3.2. Health Risk Assessment

In this study, the daily exposure and reference doses were utilized to calculate the CR and HQ of HMs of the six types of residual soils (Tables 5 and 6).

Table 5. Carcinogenic health risk index of HMs in soil.

HMs		CR _{ing}		CR _{derm}		CR _{inh}		TCR	
		Adult	Child	Adult	Child	Adult	Child	Adult	Child
As	Min	3.08 × 10 ⁻⁶	5.51 × 10 ⁻⁶	3.31 × 10 ⁻⁹	1.53 × 10 ⁻⁹	3.00 × 10 ⁻⁷	3.76 × 10 ⁻⁷	3.39 × 10 ⁻⁶	5.88 × 10 ⁻⁶
	Max	2.12 × 10 ⁻²	3.78 × 10 ⁻²	2.27 × 10 ⁻⁵	1.05 × 10 ⁻⁵	2.06 × 10 ⁻³	2.59 × 10 ⁻³	2.33 × 10 ⁻²	4.04 × 10 ⁻²
	Avg	2.12 × 10 ⁻³	3.79 × 10 ⁻³	2.27 × 10 ⁻⁶	1.05 × 10 ⁻⁶	2.06 × 10 ⁻⁴	2.59 × 10 ⁻⁴	2.32 × 10 ⁻³	4.05 × 10 ⁻³
Hg	Min	3.47 × 10 ⁻¹³	6.20 × 10 ⁻¹³	3.70 × 10 ⁻¹⁷	1.71 × 10 ⁻¹⁷	1.39 × 10 ⁻¹⁷	1.74 × 10 ⁻¹⁷	3.47 × 10 ⁻¹³	6.20 × 10 ⁻¹³
	Max	3.51 × 10 ⁻¹¹	6.27 × 10 ⁻¹¹	3.74 × 10 ⁻¹⁵	1.73 × 10 ⁻¹⁵	1.40 × 10 ⁻¹⁵	1.75 × 10 ⁻¹⁵	3.51 × 10 ⁻¹¹	6.27 × 10 ⁻¹¹
	Avg	6.15 × 10 ⁻¹²	1.10 × 10 ⁻¹¹	6.56 × 10 ⁻¹⁶	3.03 × 10 ⁻¹⁶	2.45 × 10 ⁻¹⁶	3.08 × 10 ⁻¹⁶	6.15 × 10 ⁻¹²	1.10 × 10 ⁻¹¹
Cd	Min	3.53 × 10 ⁻⁸	6.31 × 10 ⁻⁸	3.89 × 10 ⁻¹²	1.80 × 10 ⁻¹²	1.41 × 10 ⁻⁹	1.77 × 10 ⁻⁹	3.67 × 10 ⁻⁸	6.48 × 10 ⁻⁸
	Max	8.62 × 10 ⁻⁴	1.54 × 10 ⁻³	9.49 × 10 ⁻⁸	4.38 × 10 ⁻⁸	3.44 × 10 ⁻⁵	4.31 × 10 ⁻⁵	8.96 × 10 ⁻⁴	1.58 × 10 ⁻³
	Avg	6.65 × 10 ⁻⁵	1.19 × 10 ⁻⁴	7.33 × 10 ⁻⁹	3.39 × 10 ⁻⁹	2.66 × 10 ⁻⁶	3.33 × 10 ⁻⁶	6.92 × 10 ⁻⁵	1.22 × 10 ⁻⁴
Cu	Min	-	-	-	-	-	-	-	-
	Max	-	-	-	-	-	-	-	-
	Avg	-	-	-	-	-	-	-	-
Ni	Min	2.58 × 10 ⁻⁶	4.60 × 10 ⁻⁶	1.36 × 10 ⁻¹⁰	6.27 × 10 ⁻¹¹	2.57 × 10 ⁻⁶	3.22 × 10 ⁻⁶	5.15 × 10 ⁻⁶	7.83 × 10 ⁻⁶
	Max	1.30 × 10 ⁻⁴	2.32 × 10 ⁻⁴	6.84 × 10 ⁻⁹	3.16 × 10 ⁻⁹	1.30 × 10 ⁻⁴	1.62 × 10 ⁻⁴	2.59 × 10 ⁻⁴	3.94 × 10 ⁻⁴
	Avg	3.01 × 10 ⁻⁵	5.37 × 10 ⁻⁵	1.58 × 10 ⁻⁹	7.32 × 10 ⁻¹⁰	3.00 × 10 ⁻⁵	3.76 × 10 ⁻⁵	6.01 × 10 ⁻⁵	9.13 × 10 ⁻⁵
Pb	Min	5.31 × 10 ⁻⁹	9.49 × 10 ⁻⁹	2.80 × 10 ⁻¹²	1.29 × 10 ⁻¹²	4.24 × 10 ⁻¹⁰	5.31 × 10 ⁻¹⁰	5.74 × 10 ⁻⁹	1.00 × 10 ⁻⁸
	Max	9.67 × 10 ⁻⁶	1.73 × 10 ⁻⁵	5.10 × 10 ⁻⁹	2.35 × 10 ⁻⁹	7.72 × 10 ⁻⁷	9.68 × 10 ⁻⁷	1.04 × 10 ⁻⁵	1.82 × 10 ⁻⁵
	Avg	1.06 × 10 ⁻⁶	1.89 × 10 ⁻⁶	5.58 × 10 ⁻¹⁰	2.58 × 10 ⁻¹⁰	8.46 × 10 ⁻⁸	1.06 × 10 ⁻⁷	1.14 × 10 ⁻⁶	2.00 × 10 ⁻⁶

Note:“-” Avgs that there is no such data.

The CR index analysis showed that, for both adults and children, the order of different exposures was CR_{ing} > CR_{inh} > CR_{derm}, with oral intake identified as the primary CR route. The risk hierarchy for various elements in adults and children was As > Cd > Ni > Pb > Hg. Both oral intake and respiratory inhalation of As presented a CR for adults and children, whereas skin exposure was within acceptable limits. Hg intake through all routes was <10⁻⁶, indicating no CR to the human body. Children exhibited CR for Cd based on average oral intake values, while both adults and children faced CRs for Ni at specific sampling points, considering maximum values of oral intake and respiratory inhalation. The average values of oral intake of Pb and Ni fall within the range of 10⁻⁶–10⁻⁴, which is deemed acceptable. Considering both total cancer risk and the preceding analysis, As posed a CR, Cd posed a CR specifically for children, and Ni and Pb remained within acceptable limits. Hg did not present a CR for human beings.

Table 6. Non-carcinogenic health risk index of soil HMs.

Heavy Metal		HQ _{ing}		HQ _{derm}		HQ _{inh}		HI	
		Adult	Child	Adult	Child	Adult	Child	Adult	Child
As	Min	2.00×10^{-2}	1.43×10^{-1}	5.19×10^{-6}	9.60×10^{-6}	1.94×10^{-4}	9.75×10^{-4}	2.02×10^{-2}	1.44×10^{-1}
	Max	1.37×10^2	9.81×10^2	3.57×10^{-2}	6.60×10^{-2}	1.34×10^0	6.70×10^0	1.39×10^2	9.88×10^2
	Avg	1.37×10^1	9.81×10^0	3.57×10^{-3}	6.60×10^{-3}	1.34×10^{-1}	6.70×10^{-1}	1.39×10^1	9.88×10^1
Hg	Min	1.13×10^{-5}	8.04×10^{-5}	4.20×10^{-9}	7.76×10^{-9}	6.42×10^{-7}	3.22×10^{-6}	1.19×10^{-5}	8.36×10^{-5}
	Max	1.14×10^{-3}	8.12×10^{-3}	4.24×10^{-7}	7.84×10^{-7}	6.48×10^{-5}	3.25×10^{-4}	1.20×10^{-3}	8.45×10^{-3}
	Avg	1.99×10^{-4}	1.42×10^{-3}	7.44×10^{-8}	1.37×10^{-7}	1.14×10^{-5}	5.70×10^{-5}	2.11×10^{-4}	1.48×10^{-3}
Cd	Min	1.69×10^{-5}	1.21×10^{-4}	1.80×10^{-7}	3.33×10^{-7}	6.74×10^{-6}	3.38×10^{-5}	2.38×10^{-5}	1.55×10^{-4}
	Max	4.12×10^{-1}	2.94×10^0	4.39×10^{-3}	8.12×10^{-3}	1.64×10^{-1}	8.24×10^{-1}	5.81×10^{-1}	3.78×10^0
	Avg	3.18×10^{-2}	2.27×10^{-1}	3.39×10^{-4}	6.27×10^{-4}	1.27×10^{-2}	6.37×10^{-2}	4.49×10^{-2}	2.92×10^{-1}
Cu	Min	7.72×10^{-5}	5.52×10^{-4}	8.19×10^{-9}	1.51×10^{-8}	1.03×10^{-6}	5.15×10^{-6}	7.83×10^{-5}	5.57×10^{-4}
	Max	8.75×10^{-2}	6.25×10^{-1}	9.29×10^{-6}	1.72×10^{-5}	1.16×10^{-3}	5.84×10^{-3}	8.87×10^{-2}	6.31×10^{-1}
	Avg	1.32×10^{-2}	9.44×10^{-2}	1.40×10^{-6}	2.59×10^{-6}	1.76×10^{-4}	8.81×10^{-4}	1.34×10^{-2}	9.53×10^{-2}
Ni	Min	2.21×10^{-4}	1.58×10^{-3}	2.29×10^{-8}	4.23×10^{-8}	3.27×10^{-6}	1.64×10^{-5}	2.24×10^{-4}	1.60×10^{-3}
	Max	1.11×10^{-2}	7.96×10^{-2}	1.15×10^{-6}	2.13×10^{-6}	1.65×10^{-4}	8.26×10^{-4}	1.13×10^{-2}	8.04×10^{-2}
	Avg	2.58×10^{-3}	1.84×10^{-2}	2.67×10^{-7}	4.93×10^{-7}	3.81×10^{-5}	1.91×10^{-4}	2.62×10^{-3}	1.86×10^{-2}
Pb	Min	5.21×10^{-4}	3.72×10^{-3}	5.52×10^{-8}	1.02×10^{-7}	1.39×10^{-5}	6.95×10^{-5}	5.35×10^{-4}	3.79×10^{-3}
	Max	9.48×10^{-1}	6.78×10^0	1.01×10^{-4}	1.86×10^{-4}	2.52×10^{-2}	1.26×10^{-1}	9.74×10^{-1}	6.90×10^0
	Avg	1.04×10^{-1}	7.42×10^{-1}	1.10×10^{-5}	2.04×10^{-5}	2.76×10^{-3}	1.39×10^{-2}	1.07×10^{-1}	7.56×10^{-1}

The exposure routes for HQ demonstrated an order of $HQ_{ing} > HQ_{inh} > HQ_{derm}$ for both adults and children, highlighting oral intake as the predominant route of HQ risk. The order of exposure risk of different HQ elements in adults was $As > Pb > Cu > Cd > Ni > Hg$, whereas in children it was $As > Pb > Cd > Cu > Ni > Hg$. The average value of As in oral intake and the maximum value of respiratory inhalation in both adults and children was >1 , with the maximum value reaching 981 in children. This indicates significant adverse effects of As on human health, particularly affecting children through oral intake and respiratory inhalation. In contrast, the maximum oral intake of Cd and Pb in children was >1 , representing a non-CR to the human body. Other HMs exhibited values of <1 across different exposure pathways, indicating a weak impact on human health. In conclusion, it is imperative to prioritize the assessment of As pollution status and specific areas with high Cd and Pb levels in the study area. This focus is crucial to avoid adverse effects on residents, especially children. These findings serve as a foundational basis for subsequent site pollution control measures [57].

3.4. Spatial Distribution Characteristics of HMs in Soil

The inverse-distance weighting method serves as a primary tool for analyzing the overall trend of changes in surface source pollution [58,59]. To enhance the visual representation of the spatial distribution of each element, logarithmic processing was applied to the HM concentrations. ArcMAP10.8 was used to interpolate the six elements using the inverse-distance weighting method, leading to the creation of a spatial distribution map illustrating the HM pollution characteristics of the residual soil in the study area. Within areas A, B, and D, all element contents were low. Area C exhibited high values for As and Cu in some sampling points. Area G had a high value for Hg in one sampling point. Area F showed high values for Cd and Cu in some sampling points. Area H had high values at some sampling points for Hg, Ni, and Pb in area H. These high-value sampling points for each element were predominantly concentrated in the sedimentation tank, dewatering tank, and residue deposit. Specifically, the raw-ore yard, dewatering tank, and analysis laboratory displayed high concentrations of As, Cd, and Cu. The high-value points for Hg, Ni, and Pb were primarily located in the residue deposits (Figure 4). Li et al. [60] observed that HMs can easily penetrate the soil environment through direct discharge, rainwater scouring, and soil infiltration. This can result in localized high levels of HMs caused by waste residue and wastewater.

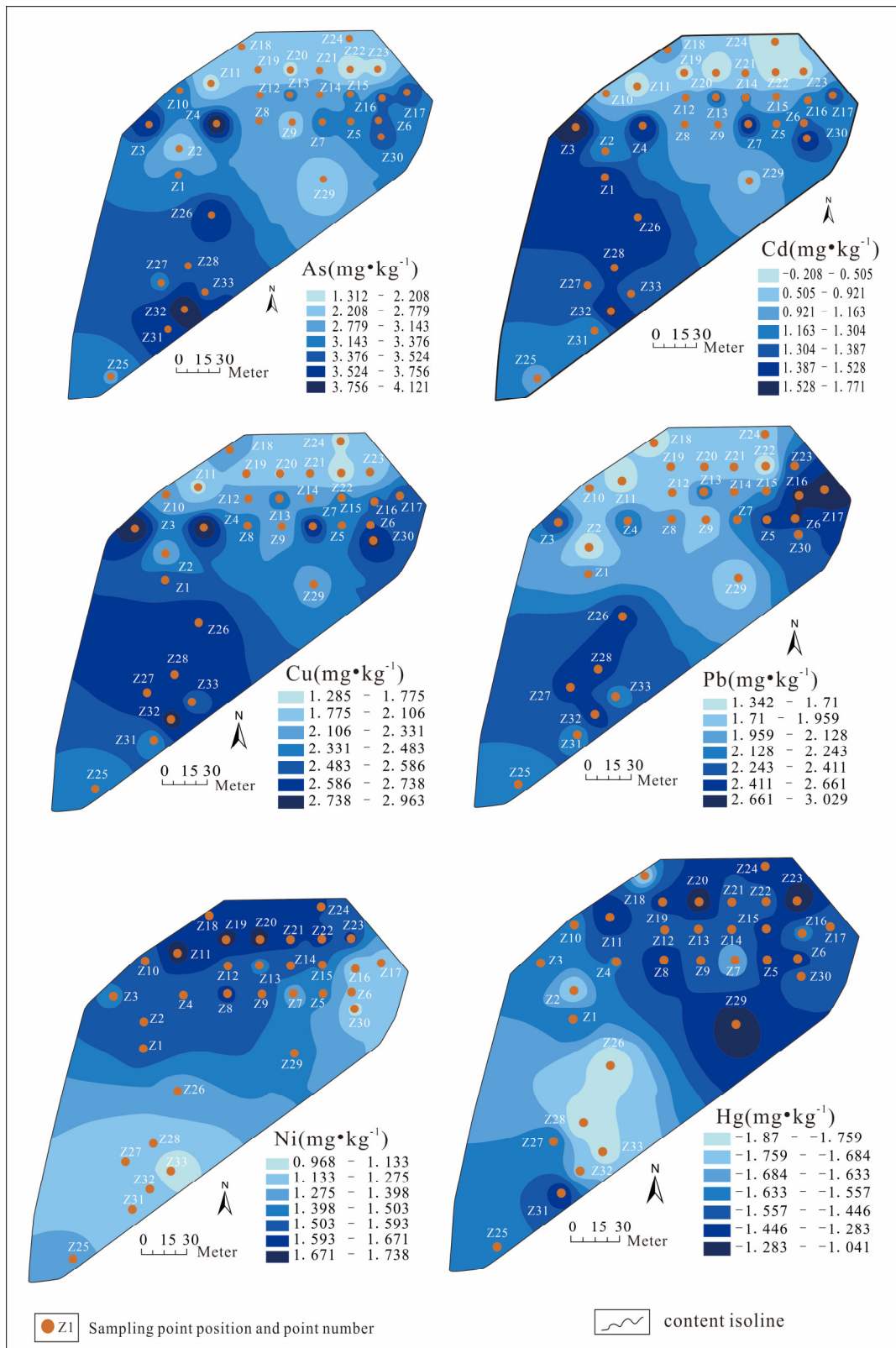


Figure 4. Characteristic distribution map of soil heavy metal(loid) content.

3.5. Source Analysis of HMs

In recent years, due to urban reforms, the relocation of numerous industrial enterprises has become a prevalent practice, emphasizing the crucial importance of re-purposing

abandoned industrial land. Industrial and mining areas present a high risk of HM pollution, posing potential health hazards for future users of the site [61]. Identifying the sources of HM pollution is particularly important for mitigating these risks.

Soil evaluations have consistently identified As and Cd as primary pollutants in this study. Surface water analysis indicated elevated levels of Cd, Cu, Pb, and pH, surpassing the permissible discharge concentrations of sewage. Groundwater exhibited significant contamination, particularly with As (93 times), followed by Cd and Ni. Research has documented HM pollution in both surface water and groundwater within industrial and mining areas and their surrounding regions, with excessive concentrations of elements such as As, Pb, and Cd [62–64], attributed to mineral processing plants specializing in Zn, Cu, and Sn ore flotation. The primary trace elements in these ores include Cd, Pb, As, Cu, and Ni [65,66].

3.5.1. Relationships between HM Concentrations and Soil Physical and Chemical Properties

The study area is situated in a geological setting characterized by high levels of Cd, with predominant limestone exposures. The high Cd content in the soil can be attributed to the weathering of carbonate rocks [67,68]. Additionally, this weathering process tends to facilitate the enrichment of other elements such as Pb, Zn, As, and Ni [69]. As, Pb, Ni, and Cu in soil primarily originate from the parent rock, with Ni also originating from the red soil [70–73]. Notably, the predominant soil traits in the region include a heavy texture and clay content [74]. Clay minerals such as kaolinite and montmorillonite facilitate the adsorption of HMs, leading to their substantial and stable accumulation in this area [75]. Regional soil samples display a pH of 2.65–8.91, with an average of 5.87, which is weakly acidic. Human activities, particularly industrial processes (flotation processes), contribute to a reduction in soil pH [76,77], impacting the migration and enrichment of HM pollutants [78–80]. For example, soil acidification leads to a significant increase in the migration rates of Cd and Pb in areas with residual industrial facilities [81,82].

3.5.2. Correlation between Different Elements across Various Media

The interrelationships among HMs can provide insights into their sources and migration patterns. A significant correlation between two metals implies a similar origin [83]. Figure 5 illustrates the relationships between different element combinations (As, Cd, Pb and Cu) in various media. Utilizing a linear model, the concentrations of HMs were fitted to derive correlation coefficients across different media within the study area [84].

The correlation coefficients between Cd and As, Cu, Pb and Cu in the soil and surface water, between As and Cd, Cu, Pb and Cu in the soil and groundwater, and between Cd, Cu, Pb, Cu and Pb in surface water and groundwater are all greater than 0.8. Higher correlation coefficients indicate that HMs share the same origin and similar geochemical behaviors. Elements with similar properties and migration behaviors may vertically migrate during the leaching process, suggesting a potential common source. As, Cd, and Pb are associated with Pb–Zn ore and are linked to the weathering and leaching of wastewater, tailings, and waste minerals [85,86]. As, being widely distributed in the environment, exhibits increased mobility in aquatic environments during heavy rainfall [87–89]. Soluble HMs such as As, Cd, Pb, and Cu enter the topsoil and water systems under the influence of rainwater [90,91]. The migration of HMs impacts regional-scale groundwater pollution, becoming a crucial factor affecting the health and safety of the surrounding population [92].

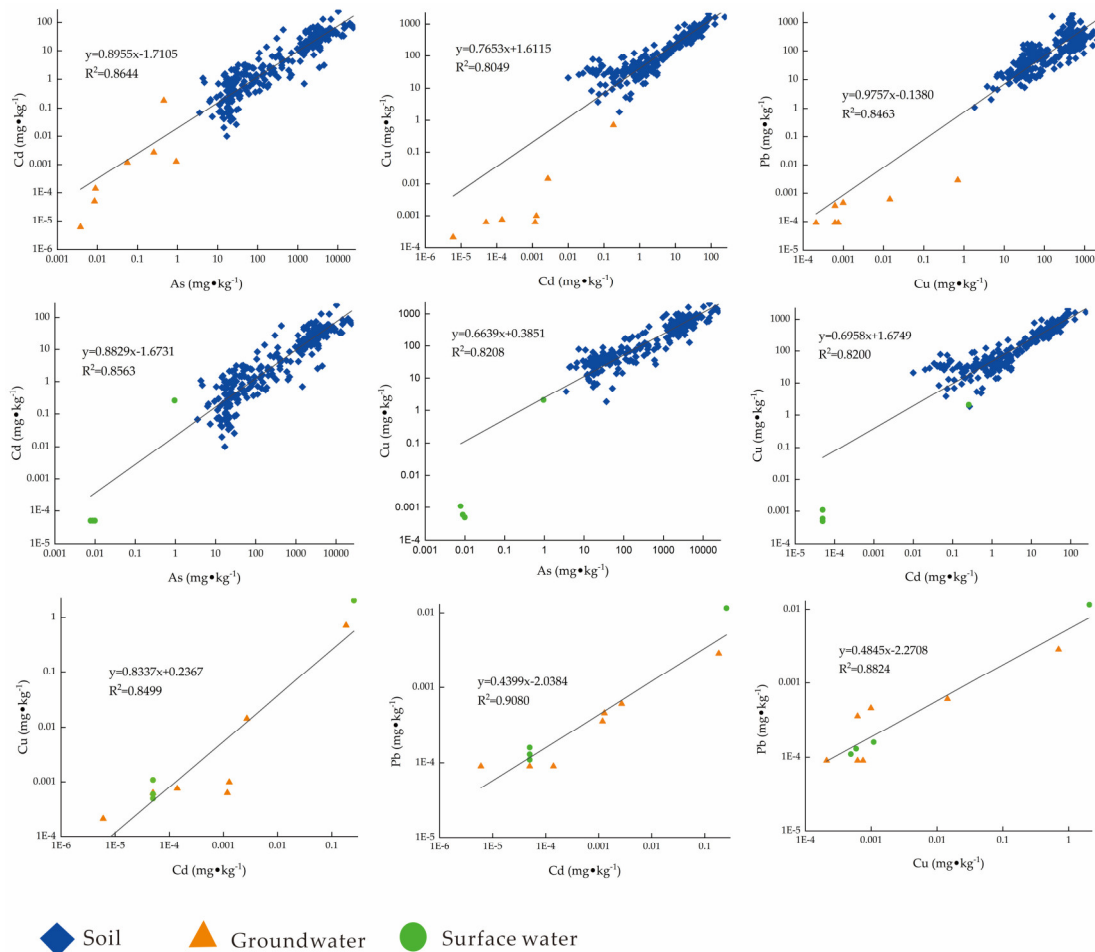


Figure 5. Relationship between heavy metal(loid) content in soil, surface water, and groundwater.

4. Conclusions

(1) The soil in the study area is acidic because of the prolonged operation of mineral processing activities. The average HM concentrations in the soil were higher than those of the background values of the soil in Yunnan Province. Spatially, the CV of the surface soil follows the order As > Pb > Cd > Cu > Hg > 1 > Ni, indicating significant variations in the spatial distribution of these elements and the possibility of anthropogenic pollution. Surface water analysis revealed elevated levels of Cd, Cu, Pb, and pH, exceeding the permissible discharge concentrations of sewage. On-site groundwater exceeded the Class III water quality standard for the parameters of pH, As, and Cd; however, the groundwater in the surrounding areas met standard requirements.

(2) The results from the P_i and P_N pollution indices indicate a consistent average pollution index in the order As > Pb > Cd > Ni > Cu > Hg. Cd requires careful consideration in future assessments as it is nearing the warning level.

(3) The health risk assessment highlights the vulnerability of children to HMs, with oral intake identified as the primary exposure route. As poses a CR, and Cd poses a CR, specifically to children. Focused attention on As, Cd, and Pb in specific areas is crucial to mitigate HQ risks to residents, particularly children. Therefore, this site is subject to soil remediation and treatment as a residential site.

(4) The spatial distribution analysis reveals concentrated high-value points in the waste slag yard, indicating a trend of concentrated distribution and compound pollution. These areas merit special attention in subsequent stages of development. Source analysis indicates that human activities and soil parent materials are the primary contributors to HM pollution in the study area.

Supplementary Materials: The following supporting information can be downloaded at: <https://www.mdpi.com/article/10.3390/min14030253/s1>, Table S1: List of Analytical Method Quality Parameters; Table S2: Risk screening values for soil contamination of Construction land. d (mg/kg); Table S3: Classification criteria for the assessment of soil heavy metal(loid) pollution assessment.; Table S4: Parameter values of health risk assessment model. [48]; Table S5. Reference dose (RfD) and slope factor (SF) of different exposure routes [93,94].

Author Contributions: Conceptualization, Y.Z. and W.L.; methodology, Y.Z. and W.L.; software, W.L.; validation, Y.Z. formal analysis, W.L. and Y.Z. investigation, P.W., W.L. and C.S.; resources, Y.Z. and P.W.; data curation, P.W., W.L. and C.S.; writing—original draft preparation, W.L.; writing—review and editing, Y.Z. and W.L.; visualization, W.L.; supervision, Y.Z. and P.W.; project administration, Y.Z. and P.W.; funding acquisition, Y.Z. All authors have read and agreed to the published version of the manuscript.

Funding: This research was funded by the Ten Thousand Talent Program of Yunnan Province (grant no.YNWR-QNBJ-2019-157),the projects of the YM Lab (2011),the Innovation Team of the Yunnan Province (2008 and 2012).

Data Availability Statement: The dataset used in this study is not publicly available due to a data privacy agreement with the Kunming Geological Exploration Institute of China Metallurgical Geology Bureau. However, it can be obtained from the corresponding author upon reasonable request.

Acknowledgments: We thank yinxian Song (Kunming University of Science and Technology) for careful guidance and assistance in the writing process of the article.

Conflicts of Interest: The authors declare no conflicts of interest.

Abbreviations

CV	coefficient of variation
HMs	Heavy metal(loid)s
CR	Carcinogenic risk
TCR	Multi-element total carcinogenic risk
SD	Standard deviation

References

1. Cui, L.; Wang, X.L.N.; Li, J.; Gao, X.Y.; Zhang, J.W.; Liu, Z.T. Ecological and health risk assessments and water quality criteria of heavy metals in the Haihe River. *Environ. Pollut.* **2021**, *290*, 1177971. [[CrossRef](#)]
2. Li, H.; Yao, J.; Min, N.; Chen, Z.H.; Li, M.M.M.; Pang, W.C.; Liu, B.; Cao, Y.; Men, D.Y.; Duran, R. Comprehensive evaluation of metal(loid)s pollution risk and microbial activity characteristics in non-ferrous metal smelting contaminated site. *J. Clean. Prod.* **2022**, *344*, 130999. [[CrossRef](#)]
3. Luo, X.H.; Wu, C.; Lin, Y.C.; Li, W.C.; Deng, M.; Tan, J.Q.; Xue, S.G. Soil heavy metal pollution from Pb/Zn smelting regions in China and the remediation potential of biomineralization. *J. Environ. Sci.* **2023**, *125*, 662–677. [[CrossRef](#)]
4. Yan, K.; Wang, H.Z.; Lan, Z.; Zhou, J.H.; Fu, H.Z.; Wu, L.S.; Xu, J.M. Heavy metal pollution in the soil of contaminated sites in China: Research status and pollution assessment over the past two decades. *J. Clean. Prod.* **2022**, *373*, 133780. [[CrossRef](#)]
5. Zhang, Y.B.; Zhang, Q.L.; Chen, W.F.; Shi, W.W.; Cui, Y.L.; Chen, L.L.; Shao, J.L. Hydrogeochemical analysis and groundwater pollution source identification based on self-organizing map at a contaminated site. *J. Clean. Prod.* **2023**, *616*, 128839. [[CrossRef](#)]
6. Fry, L.K.; Wheeler, A.C.; Gillings, M.M.; Flegal, R.A.; Taylor, M.P. Anthropogenic in some areas of residential environments from smelter As, Cu and Pb emissions: Implications for human health. *Environ. Pollut.* **2020**, *262*, 114235. [[CrossRef](#)]
7. Khan, S.; Naushad, M.; Lima, C.E.; Zhang, S.; Sabry, M.S.; Jörg, R. Global soil pollution by toxic elements: Current status and future perspectives on the risk assessment and remediation strategies—A review. *J. Hazard. Mater.* **2021**, *417*, 126039. [[CrossRef](#)]
8. Tomiyama, S.; Igarashi, T.; Tabelin, B.C.; Pawit, T.; Hiroyuki, I. Acid mine drainage sources and hydrogeochemistry at the Yatani mine, Yamagata, Japan: A geochemical and isotopic study. *J. Contam. Hydrol.* **2019**, *225*, 103502. [[CrossRef](#)]
9. Park, I.; Tabelin, B.C.; Jeon, S.; Li, X.; Seno, K.; Ito, M.; Hiroyoshi, N. A review of recent strategies for acid mine drainage prevention and mine tailings recycling. *Chemosphere* **2019**, *219*, 588–606. [[CrossRef](#)]
10. Silwamba, M.; Ito, M.; Hiroyoshi, N.; Tabelin, C.B.; Fukushima, T.; Park, I.; Jeon, S.; Igarashi, T.; Sato, T.; Nyambe, I.A. Detoxification of lead-bearing zinc plant leach residues from Kabwe, Zambia by coupled extraction-cementation method. *J. Environ. Chem. Eng.* **2020**, *8*, 104197. [[CrossRef](#)]
11. Baltazar, C.T.; Asuka, U.; Shingo, T.; Mylah, V.; Theerayut, P.; Marthias, S.; Sanghee, J.; Ilhwan, P.; Takahiko, A.; Toshifumi, I. Geochemical audit of a historical tailings storage facility in Japan: Acid mine drainage formation, zinc migration and mitigation strategies. *J. Hazard. Mater.* **2022**, *438*, 129453.

12. Isildar, A.; van Hullebusch, E.D.; Lenz, M.; Du Laing, G.; Marra, A.; Cesaro, A.; Panda, S.; Akcil, A.; Kucuker, M.A.; Kuchta, K. Biotechnological strategies for the recovery of valuable and critical raw materials from waste electrical and electronic equipment (WEEE)—A review. *J. Hazard. Mater.* **2019**, *362*, 467–481. [[CrossRef](#)]
13. Hussein, M.; Yoneda, K.; Mohd-Zaki, Z.; Amir, A.; Othman, N. Heavy metals in leachate, impacted soils and natural soils of different landfills in Malaysia: An alarming threat. *Chemosphere* **2021**, *267*, 128874. [[CrossRef](#)]
14. Liao, J.B.; Qian, X.; Liu, F.; Deng, S.; Lin, H.; Liu, X.H.; Wei, C.H. Multiphase distribution and migration characteristics of heavy metals in typical sandy intertidal zones: Insights from solid-liquid partitioning. *Ecotoxicol. Environ.* **2021**, *208*, 111674. [[CrossRef](#)]
15. Qiu, H.; Lou, Z.Y.; Gu, X.Y.; Sun, Y.Y.; Wang, J.; Zhang, W.; Cao, X.D. Smart 6S roadmap for deciphering the migration and risk of heavy metals in soil and groundwater systems at brownfield sites nationwide in China. *Sci. Bull.* **2022**, *67*, 1295–1299. [[CrossRef](#)]
16. Ciarkowska, K.; Gambus, F. Building a quality index for soils impacted by proximity to an industrial complex using statistical and data-mining methods. *Sci. Total Environ.* **2020**, *740*, 140161. [[CrossRef](#)]
17. Ali Zerrouki, A.; Melila, M. Evaluation of soil contamination by heavy metals in the vicinity of Boucaid Mine, Ouarsenis (N.O. Algeria). *Soil Sediment Contam.* **2021**, *30*, 924–942. [[CrossRef](#)]
18. Baieta, R.; Mihaljevič, M.; Ettler, V.; Vaněk, A.; Penížek, V.; Trubač, J.; Kříbek, B.; Ježek, J.; Svoboda, M.; Sracek, O.; et al. Depicting the historical pollution in a Pb–Zn mining/smelting site in Kabwe (Zambia) using tree rings. *J. Afr. Earth Sci.* **2021**, *181*, 104246. [[CrossRef](#)]
19. Nguyen, M.H.; Van, H.T.; Thang, P.Q.; Hoang, T.H.N.; Dao, D.C.; Nguyen, C.L.; Nguyen, L.H. Level and potential risk assessment of soil contamination by trace metal from mining activities. *Soil Sediment Contam.* **2021**, *30*, 92–106. [[CrossRef](#)]
20. Peng, J.Y.; Zhang, S.; Han, Y.Y.; Bate, B.; Ke, H.; Chen, Y.M. Soil heavy metal pollution of industrial legacies in China and health risk assessment. *Sci. Total Environ.* **2022**, *816*, 151632. [[CrossRef](#)]
21. Nyiramigisha, P.; Komariah, S. The concentration of heavy metals zinc and lead in the soil around the Putri Cempo landfill, Indonesia. *IOP Conf. Ser. Earth Environ. Sci.* **2021**, *824*, 012050. [[CrossRef](#)]
22. Augustsson, A.; Uddh Soderberg, T.; Froberg, M.; Berggren Kleja, D.B.; Astrom, M.; Svensson, P.A.; Jarsjo, J. Failure of generic risk assessment model framework to predict groundwater pollution risk at hundreds of metal contaminated sites: Implications for research needs. *Environ. Res.* **2020**, *185*, 109252. [[CrossRef](#)]
23. Li, H.X.; Li, Y.; Guo, G.H.; Li, Y.; Zhang, R.Q.; Feng, C.L.; Zhang, Y.H. Distribution, Site-Specific Water Quality Criteria, and Ecological Risk Assessment of Heavy Metals in Surface Water in Fen River, China. *Toxics* **2023**, *11*, 704. [[CrossRef](#)]
24. Topal, M.; Arslan, T. Phytoremediation of priority substances (Pb and Ni) by *Phragmites australis* exposed to poultry slaughterhouse wastewater. *Int. J. Phytoremediat.* **2020**, *22*, 857–862. [[CrossRef](#)]
25. Bai, Z.Y.; Wu, F.Z.; He, Y.P.; Han, Z.W. Pollution and risk assessment of heavy metals in Zuoxiguo antimony mining area, southwest China. *Environ. Pollut. Bioavailab.* **2023**, *35*, 2156397. [[CrossRef](#)]
26. Jiang, Z.J.; Yang, S.Z.; Luo, S. Source analysis and health risk assessment of heavy metals in agricultural land of multi-mineral mining and smelting area in the Karst region—A case study of Jichangpo Town, Southwest China. *Heliyon* **2023**, *9*, e17246. [[CrossRef](#)]
27. Liu, H.J.; Xie, J.; Cheng, Z.F.; Wu, X.L. Characteristics, Chemical Speciation and Health Risk Assessment of Heavy Metals in Paddy Soil and Rice around an Abandoned High-Arsenic Coal Mine Area, Southwest China. *Minerals* **2023**, *13*, 629. [[CrossRef](#)]
28. Zhang, Q.; Han, G.L.; Liu, M.; Liang, T. Spatial distribution and controlling factors of heavy metals in soils from Puding Karst Critical Zone Observatory, southwest China. *Environ. Earth Sci.* **2019**, *78*, 279. [[CrossRef](#)]
29. Laniyan, T.A.; Morakinyo, O.M. Environmental sustainability and prevention of heavy metal pollution of some geo-materials within a city in southwestern Nigeria. *Heliyon* **2021**, *7*, e06796. [[CrossRef](#)]
30. Davis, A.; Olsen, R.L.; Walker, D.R. Distribution of metals between water and entrained sediment in streams impacted by acid mine discharge, Clear Creek, Colorado, U.S. *Appl. Geochem.* **1991**, *6*, 333–348. [[CrossRef](#)]
31. Zhang, W.; Long, J.H.; Wei, Z.Y.; Alakangas, L. Vertical distribution and historical loss estimation of heavy metals in an abandoned tailings pond at HTM coppermine, northeastern China. *Environ. Earth Sci.* **2016**, *75*, 11–13. [[CrossRef](#)]
32. Li, Z.; Deblon, J.; Zu, Y.; Colinet, G.; Li, B.; He, Y.M. Geochemical Baseline Values Determination and Evaluation of Heavy Metal Contamination in Soils of Lanping Mining Valley (Yunnan Province, China). *Int. J. Environ. Res. Public Health* **2019**, *16*, 4686. [[CrossRef](#)] [[PubMed](#)]
33. Chen, W.D.; Yao, W.W.; Huang, Z.X.; Ying, Q.C.; He, Z.W. Assessment of Soil Trace Metal Pollution in the Xuejiping Mine Area, Yunnan, China. *Clean—Soil Air Water* **2021**, *49*, 2000093. [[CrossRef](#)]
34. Xu, S.C.; Huang, Z.; Huang, J.X.; Wu, S.; Yan, D.; Chen, Z.; Yang, B.C.; Xu, Y.Q.; Liu, N.Q.; Gong, Q.J. Environmental Pollution Assessment of Heavy Metals in Soils and Crops in Xinping Area of Yunnan Province, China. *Appl. Sci.* **2023**, *13*, 10810. [[CrossRef](#)]
35. HJ25.2-2014; Technical Guidelines for Environmental Site Environmental Monitoring. Ministry of Ecology and Environment of the People’s Republic of China: Beijing, China, 2014.
36. HJ-T91-2002; Technical Specification for Surface Water and Sewage Monitoring. Ministry of Ecology and Environment of the People’s Republic of China: Beijing, China, 2002.
37. HJ 493-2009; Water Quality sampling—Technical Regulation of the Preservation and handling of Samples. Ministry of Ecology and Environment of the People’s Republic of China: Beijing, China, 2009.
38. HJ/T166-2004; Technical Specification for Soil Environmental Monitoring. Ministry of Ecology and Environment of the People’s Republic of China: Beijing, China, 2002.

39. GB-15618-2018; Soil Environment Quality Risk Control Standard for Soil Contamination of Agriculture Land. Ministry of Ecology and Environment of the People's Republic of China: Beijing, China, 2018; State Administration of Market Regulation: Beijing, China, 2018.
40. Fan, C.Z.; Liu, Y.B.; Liu, C.H.; Zhao, W.B.; Hao, N.X.; Guo, W.; Yuan, J.H.; Zhao, J.J. Water quality characteristics, sources, and assessment of surface water in an industrial mining city, southwest of China. *Environ. Monit. Assess.* **2022**, *194*, 25. [[CrossRef](#)] [[PubMed](#)]
41. Ren, J.; Zhan, W.; Lu, G.C. Environmental Assessment of Heavy Metals in the Typical Vegetable Field and Irrigation Sediment in Xijiang River Basin, China: Spatial Distribution and Ecological Risk. *Water Air Soil Pollut.* **2023**, *234*, 558. [[CrossRef](#)]
42. An, M.Y.; Song, Y.W.; Jiang, J.Y.; Fu, G.W.; Wang, Y.; Wan, X.M. Water Quality Evaluation, Spatial Distribution Characteristics, and Source Analysis of Pollutants in Wanquan River, China. *Appl. Sci.* **2023**, *13*, 7982. [[CrossRef](#)]
43. Kumi, M.; Anku, W.W.; Antwi, B.Y.; Penny, P.G. Evaluation of the suitability of integrated bone char- and biochar-treated groundwater for drinking using single-factor, Nemerow, and heavy metal pollution indexes. *Environ. Monit. Assess.* **2023**, *195*, 647. [[CrossRef](#)]
44. Yvan, R.S.A.; Roger, T.F.T.; Mefomdjo, B.F.; Leroy, L.N.M.; Bernard, L.T.; Arsène, M. Contamination and risk assessment of trace metals and as in surface sediments from abandoned gold mining sites of Bekao, Adamawa-Cameroon. *Reg. Stud. Mar. Sci.* **2023**, *62*, 102985.
45. Siriuma, J.; Supabhorn, Y.; Panatda, P. Soil heavy metal pollution from waste electrical and electronic equipment of repair and junk shops in southern Thailand and their ecological risk. *Heliyon* **2023**, *9*, e2043.
46. Asghari, F.; Salavati, M.; Hakimi, A.S.; Shariati, F. Geochemical and environmental assessment of river sediments in the East of Gilan province (case study: Otaghvarrud, Shalmanrud, and Polrud rivers), Northern Iran. *Toxin Rev.* **2023**, *42*, 681–700. [[CrossRef](#)]
47. USEPA. *A Risk Assessment—Multi Way Exposure Spread Sheet Calculation Tool*; United States Environmental Protection Agency: Washington, DC, USA, 1999.
48. USEPA. *Risk Assessment Guidance for Superfund: Volume III—Part A. Process for Conducting Probabilistic Risk Assessment*; USEPA: Washington, DC, USA, 2001.
49. China Environmental Monitoring Station. *Background Value of Soil Elements in China*; China Environmental Press: Beijing, China, 1990.
50. Karimi, N.; Mohammad, T.; Tabatabaie, S.M.; Gholami, A. Geochemical assessment of steel smelter-impacted urban soils, Ahvaz, Iran. *J. Geochem. Explor.* **2015**, *152*, 91–109. [[CrossRef](#)]
51. GB 3838—2002; Environmental Quality Standard for Surface Water. Ministry of Ecology and Environment of the People's Republic of China: Beijing, China, 2018; State Administration of Market Regulation: Beijing, China, 2002.
52. GB 8978—1996; Integrated Wastewater Discharge Standard. The State Bureau of Quality and Technical Supervision: Beijing, China, 1996.
53. GB/T14848 2017; Standard for Groundwater Quality. Ministry of Ecology and Environment of the People's Republic of China: Beijing, China, 2018; State Administration of Market Regulation: Beijing, China, 2017.
54. USEPA. *Risk Assessment Guidance for Superfund Volume I: Human Health Evaluation Manual Supplemental Guidance*; USEPA: Washington, DC, USA, 1991.
55. Dourson, M.; Patterson, J. A 20-year perspective on the development of non-cancer risk assessment methods. *Hum. Ecol. Risk Assess.* **2003**, *9*, 1239–1252. [[CrossRef](#)]
56. Xiao, J.; Wang, L.Q.; Deng, L.; Jin, Z.D. Characteristics, sources, water quality and health risk assessment of trace elements in river water and well water in the Chinese Loess Plateau. *Sci. Total Environ.* **2019**, *650*, 2004–2012. [[CrossRef](#)] [[PubMed](#)]
57. Li, Z.Y.; Li, H.K. Research progress on heavy metal pollution and risk assessment methods in site. *Environ. Pollut.* **2021**, *43*, 1201–1204+1208.
58. Qiao, P.; Li, P.; Chen, Y.; Wei, W.; Yang, S.; Lei, M.; Chen, T. Comparison of common spatial interpolation methods for analyzing pollutant spatial distributions at contaminated sites. *Environ. Geochem. Health* **2019**, *41*, 2709–2730. [[CrossRef](#)] [[PubMed](#)]
59. Xue, S.D.; Wang, Y.Y.; Jiang, J.; Tang, L.; Xie, Y.; Gao, W.Y.; Tan, X.Y.; Zeng, J.Q. Groundwater heavy metal(loid)s risk prediction based on topsoil contamination and aquifer vulnerability at a zinc smelting site. *Environ. Pollut.* **2023**, *341*, 122939. [[CrossRef](#)]
60. Li, H.J.; Yang, Y.J.; Lv, H.M. Research and application of indium recovery process from intermediate slag of indium smelting. *World Nonferrous Met.* **2018**, 30–31.
61. Chen, T.B.; Zheng, Y.M.; Lei, M.; Huang, Z.C.; Wu, H.T.; Chen, H.; Fank, K.K.; Yu, K.; Wu, X.; Tian, Q.Z. Assessment of heavy metal pollution in surface soils of urban parks in Beijing, China. *Chemosphere* **2005**, *60*, 542–551. [[CrossRef](#)]
62. Ma, X.J.; Lu, F.; Chen, L.L.; Chen, M. Heavy metal pollution and ecological risk assessment of surface water in Guizhou manganese mining area. *Environ. Sci. Technol.* **2018**, *41*, 191–197.
63. Wu, W.H.; Zou, H.; Zhu, G.H.; Liao, Y.H.; Pan, H.T.; Xiao, Z.C.; Fan, J.; Li, L. Heavy metal pollution characteristics and health risk assessment of groundwater in a mining area in central Hunan. *J. Ecol. Rural Environ.* **2018**, *34*, 1027–1033.
64. Zheng, Y.L.; Zhu, M.; Zheng, T.; Yao, Q.; Li, H.Y.; Li, H.; Yu, Y.J. Heavy metal pollution characteristics and potential risk assessment of farmland soil and surface water in e-waste dismantling area. *Environ. Chem.* **2023**, *42*, 2946–2960.
65. Forghani, G.; Kelm, U.; Mazinani, V. Spatial distribution and chemical partitioning of potentially toxic elements in soils around Khatoon-Abad Cu Smelter, SE Iran. *J. Geochem. Explor.* **2019**, *196*, 66–80. [[CrossRef](#)]

66. Ma, W.; Song, Y.C.; Zhuang, L.L.; Wu, W. Mass transfer during hydrothermal bleaching alteration of red beds in the Lanping Basin, SW China: Implications for regional Cu(–Co) and Pb–Zn mineralization. *Ore Geol. Rev.* **2023**, *163*, 105744. [[CrossRef](#)]
67. Liu, P.F.; Wu, Z.Q.; Luo, X.R.; Wen, M.L.; Huang, L.L.; Chen, B.; Zheng, C.J.; Zhu, C.J.; Liang, R. Pollution Assessment and Source Analysis of Heavy Metals in Acidic Farmland of the Karst Region in Southern China—A Case Study of Quanzhou County. *Appl. Geochem.* **2020**, *123*, 104764. [[CrossRef](#)]
68. Li, Q.H.; Li, X.X.; Bu, C.J.; Wu, P. Distribution, risk assessment, and source apportionment of heavy metal pollution in cultivated soil of typical mining area in Southwest, China. *Environ. Toxicol. Chem.* **2023**, *42*, 888–900. [[CrossRef](#)] [[PubMed](#)]
69. Gong, Q.J.; Deng, J.; Jia, Y.J.; Tong, Y.K.; Liu, N.Q. Empirical equations to describe trace element behaviors due to rock weathering in China. *J. Geochem. Explor.* **2015**, *152*, 110–117. [[CrossRef](#)]
70. Gil-Díaz, M.; Rodríguez-Valdés, E.; Alonso, J.; Baragano, D.; Gallego, J.R.; Lobo, M.C. Nanoremediation and long-term monitoring of brownfield soil highly polluted with As and Hg. *Sci. Total Environ.* **2019**, *675*, 165–175. [[CrossRef](#)]
71. Guo, H.M.; Li, X.M.; Xiu, W.; He, W.; Cao, Y.S.; Zhang, D.; Wang, A. Controls of organic matter bioreactivity on arsenic mobility in shallow aquifers of the Hetao Basin, P.R. China. *J. Hydrol.* **2019**, *571*, 448–459. [[CrossRef](#)]
72. Jiang, H.H.; Cai, L.M.; Wen, H.H.; Luo, J. Characterizing pollution and source identification of heavy metals in soils using geochemical baseline and PMF approach. *Sci. Rep.* **2020**, *10*, 6460. [[CrossRef](#)]
73. Araújo, P.R.M.; Biondi, C.M.; do Nascimento, C.W.A.; da Silva, F.B.V.; da Silva, W.R.; da Silva, F.L.; de Melo Ferreira, D.K. Assessing the spatial distribution and ecologic and human health risks in mangrove soils polluted by Hg in northeastern Brazil. *Chemosphere* **2021**, *266*, 129019. [[CrossRef](#)] [[PubMed](#)]
74. Ke, W.S.; Zeng, J.Q.; Zhu, F.; Luo, X.H.; Feng, J.P.; He, J.; Xue, S.G. Geochemical partitioning and spatial distribution of heavy metals in soils contaminated by lead smelting. *Environ. Pollut.* **2022**, *307*, 11948. [[CrossRef](#)] [[PubMed](#)]
75. Zeng, J.Q.; Luo, X.H.; Cheng, Y.Z.; Ke, W.S.; Hartley, W.; Li, C.X.; Jiang, J.; Zhu, F.; Xue, S.G. Spatial distribution of toxic metal(loid)s at an abandoned zinc smelting site, Southern China. *J. Hazard. Mater.* **2022**, *425*, 127970. [[CrossRef](#)] [[PubMed](#)]
76. Ma, T.T.; Zhou, W.; Yang, X.; Christie, P.; Luo, Y.M. Risk Assessment of Contamination by Potentially Toxic Metals: A Case Study in the Vicinity of an Abandoned Pyrite Mine. *Minerals* **2019**, *9*, 783. [[CrossRef](#)]
77. Liu, W.; Zhang, X.X.; Zhang, W.W.; He, S.W.; Luo, S.H.; Han, J.G.; Shen, D.L. Metal-driven bacterial community variation in urban and suburban park soils of Shanghai, China. *Eur. J. Soil Biol.* **2023**, *115*, 103475. [[CrossRef](#)]
78. Qin, W.J.; Han, D.M.; Song, X.F.; Liu, S.H. Sources and migration of heavy metals in a karst water system under the threats of an abandoned Pb–Zn mine, Southwest China. *Environ. Pollut.* **2021**, *277*, 116774. [[CrossRef](#)] [[PubMed](#)]
79. Qiao, P.W.; Wang, S.; Li, J.B.; Zhao, Q.Y.; Wei, Y.; Lei, M.; Yang, J.; Zhang, Z.G. Process, influencing factors, and simulation of the lateral transport of heavy metals in surface runoff in a mining area driven by rainfall: A review. *Sci. Total Environ.* **2022**, *857*, 159119. [[CrossRef](#)]
80. Zhao, B.; Zhu, W.X.; Hao, S.F.; Hua, M.; Liao, Q.L.; Jing, Y.; Liu, L.; Gu, X.Y. Prediction heavy metals accumulation risk in rice using machine learning and mapping pollution risk. *J. Hazard. Mater.* **2023**, *448*, 130879. [[CrossRef](#)]
81. Bravo, S.; Amorós, J.A.; Pérez-de-los-Reyes, C.; García, F.J.; Moreno, M.M.; Sánchez-Ormeño, M.; Higuera, P. Influence of the soil pH in the uptake and bioaccumulation of heavy metals (Fe, Zn, Cu, Pb and Mn) and other elements (Ca, K, Al, Sr and Ba) in vine leaves, Castilla-La Mancha (Spain). *J. Geochem. Explor.* **2017**, *174*, 79–83. [[CrossRef](#)]
82. Alicja, K.; Radosław, P.; Miguel, I. Changes in soil pH and mobility of heavy metals in contaminated soils. *Eur. J. Soil Sci.* **2021**, *73*, e13203.
83. Sheng, L.L.; Hao, C.M.; Guan, S.D.; Huang, Z.B. Spatial distribution, geochemical behaviors and risk assessment of antimony in rivers around the antimony mine of Xikuangshan, Hunan Province, China. *Water Sci. Technol.* **2022**, *85*, 1141–1154. [[CrossRef](#)] [[PubMed](#)]
84. Wu, X.R. Study on Environmental Geochemical Characteristics of Heavy Metal Elements in Southwest Shandong Coal Mine Area. Ph.D. Thesis, Wuhan University of Technology, Wuhan, China, 2013.
85. Liao, Q.L.; Cui, X.D.; Huang, S.S.; Huang, B.; Ren, J.H.; Gu, X.Y.; Fan, J.; Xu, H.T. Element geochemistry of selenium-enriched soil and its main sources in Jiangsu Province. *Geol. China* **2020**, *47*, 1813–1825.
86. Cao, J.; Xie, C.Y.; Hou, Z.R. Ecological evaluation of heavy metal pollution in the soil of Pb–Zn mines. *Ecotoxicology* **2022**, *31*, 259–270. [[CrossRef](#)] [[PubMed](#)]
87. Shi, L.D.; Guo, T.; Lv, P.L.; Niu, Z.F.; Zhou, Y.J.; Tang, X.J.; Zheng, P.; Zhu, L.Z.; Zhu, Y.G.; Kappler, A.; et al. Coupled anaerobic methane oxidation and reductive arsenic mobilization in wetland soils. *Nat. Geosci.* **2020**, *13*, 799–805. [[CrossRef](#)]
88. Tran, T.H.H.; Kim, S.H.; Jo, H.Y.; Chung, J.; Lee, S. Transient behavior of arsenic in vadose zone under alternating wet and dry conditions: A comparative soil column study. *J. Hazard. Mater.* **2022**, *422*, 126957. [[CrossRef](#)] [[PubMed](#)]
89. Park, J.; Lee, D.; Kim, H.; Woo, N.C. Effects of dry and heavy rainfall periods on arsenic species and behaviour in the aquatic environment adjacent a mining area in South Korea. *J. Hazard. Mater.* **2023**, *441*, 129968. [[CrossRef](#)]
90. Kang, M.J.; Yu, S.; Jeon, S.W.; Jung, M.C.; Kwon, Y.K.; Lee, P.K.; Chae, G. Mobility of metal(loid)s in roof dusts and agricultural soils surrounding a Zn smelter: Focused on the impacts of smelter-derived fugitive dusts. *Sci. Total Environ.* **2021**, *757*, 143884. [[CrossRef](#)] [[PubMed](#)]
91. Anaman, R.; Peng, C.; Jiang, Z.C.; Liu, X.; Zhou, Z.R.; Guo, Z.H.; Xiao, X.Y. Identifying sources and transport routes of heavy metals in soil with different land uses around a smelting site by GIS based PCA and PMF. *Sci. Total Environ.* **2022**, *823*, 15375. [[CrossRef](#)]

92. Fang, H.; Wang, X.J.; Xia, D.; Zhu, J.T.; Yu, W.D.; Su, Y.M.; Zeng, J.W.; Zhang, Y.L.; Lin, X.J.; Lei, Y.T.; et al. Improvement of Ecological Risk Considering Heavy Metal in Soil and Groundwater Surrounding Electroplating Factories. *Processes* **2022**, *10*, 1267. [[CrossRef](#)]
93. Chen, J.; Shi, W.; Zhang, Y.; Song, Y. Pollution analysis and health risk spatial distribution evaluation of electroplating factory legacy sites. *Environ. Eng.* **2018**, *36*, 153–159.
94. Tao, H.; Zhang, X.; Wang, Y.; Tao, E.; Wang, F. Distribution characteristics and health risk assessment of heavy metal pollution in surface dust of Yinchuan urban area. *Environ. Chem.* **2022**, *41*, 2573–2585.

Disclaimer/Publisher’s Note: The statements, opinions and data contained in all publications are solely those of the individual author(s) and contributor(s) and not of MDPI and/or the editor(s). MDPI and/or the editor(s) disclaim responsibility for any injury to people or property resulting from any ideas, methods, instructions or products referred to in the content.